continued

(2) For a granite pluton:

$$|g''_{max}|/|g''_{min}| \leqslant 1.0.$$

Granite pluton sides slope *outwards*.

The vertical variation of density of sediments with depth in a sedimentary basin can be represented in a number of ways. Moving away from Bott's uniform density model, consideration of the variation in density in terms of exponential and hyperbolic density contrast has been given by Rao *et al.* (1993) and Rao *et al.* (1994), for example.

2.7 APPLICATIONS AND CASE HISTORIES

In this section, a limited number of case histories are described to illustrate the diversity of applications to which the gravity method can be put. Other geophysical methods are discussed as appropriate, where they have been used in conjunction with, or to contrast with, the gravity results. These other methods are explained in their respective chapters.

2.7.1 Exploration of salt domes

2.7.1.1 Mors salt dome, Denmark (waste disposal)

An original interpretation of the Bouguer anomaly (Figure 2.37) over the Mors salt dome in northern Jutland was made in 1974, five years before any seismic results were known (Sharma, 1986). The investigation was connected to a feasibility study for the safe disposal of radioactive waste in the salt dome, but the methodology is identical had the study been for hydrocarbons.

The salt dome was approximated by a sphere. The values of $\Delta g_{max} \approx 16$ mGal and the half-width ≈ 3.7 km were obtained from profiles across the feature (Figure 2.38A) used to determine the depth to the centre of mass ($z = 4.8$ km). In order to calculate the depth to the top of the sphere, an estimate of the density contrast of the salt with the surrounding material had to be made. For a density contrast ($\delta\rho$) of -0.25 Mg/m^3, this gave the radius of the sphere as 3.8 km and thus depth to the top of the sphere is about 1 km (4.8 km minus 3.8 km); with $\delta\rho = -0.2$ Mg/m^3, the radius is 4.1 km and depth to the top is 0.7 km (4.8 km -4.1 km). This was later found to be in good agreement with the seismic results (Figure 2.38B). If the salt dome approximated to a vertical cylinder of length 5300 m, depth to top 700 m, and radius 4400 m, and density contrast -0.2 Mg/m^3, the expected value of Δg_{max} is around 19 mGal, compared with an observed value of 16–18 mGal; but this is still close enough to be a reasonable approximation to the actual shape.

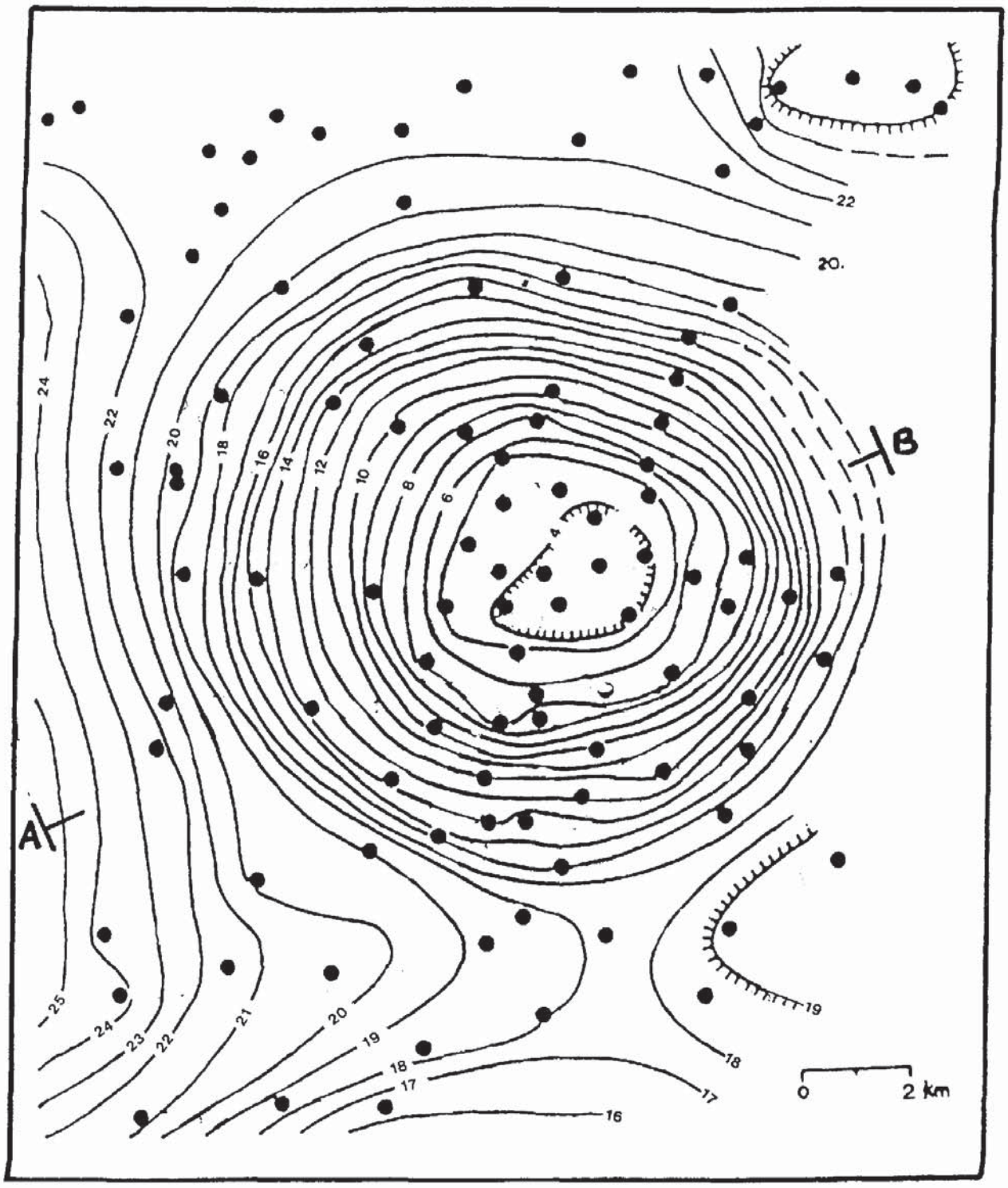

Figure 2.37 Bouguer anomaly map of the Mors salt dome, Jutland, Denmark. Solid dots represent observation points. Contour interval = 1 mGal. From Saxov (1956) and Sharma (1986), by permission

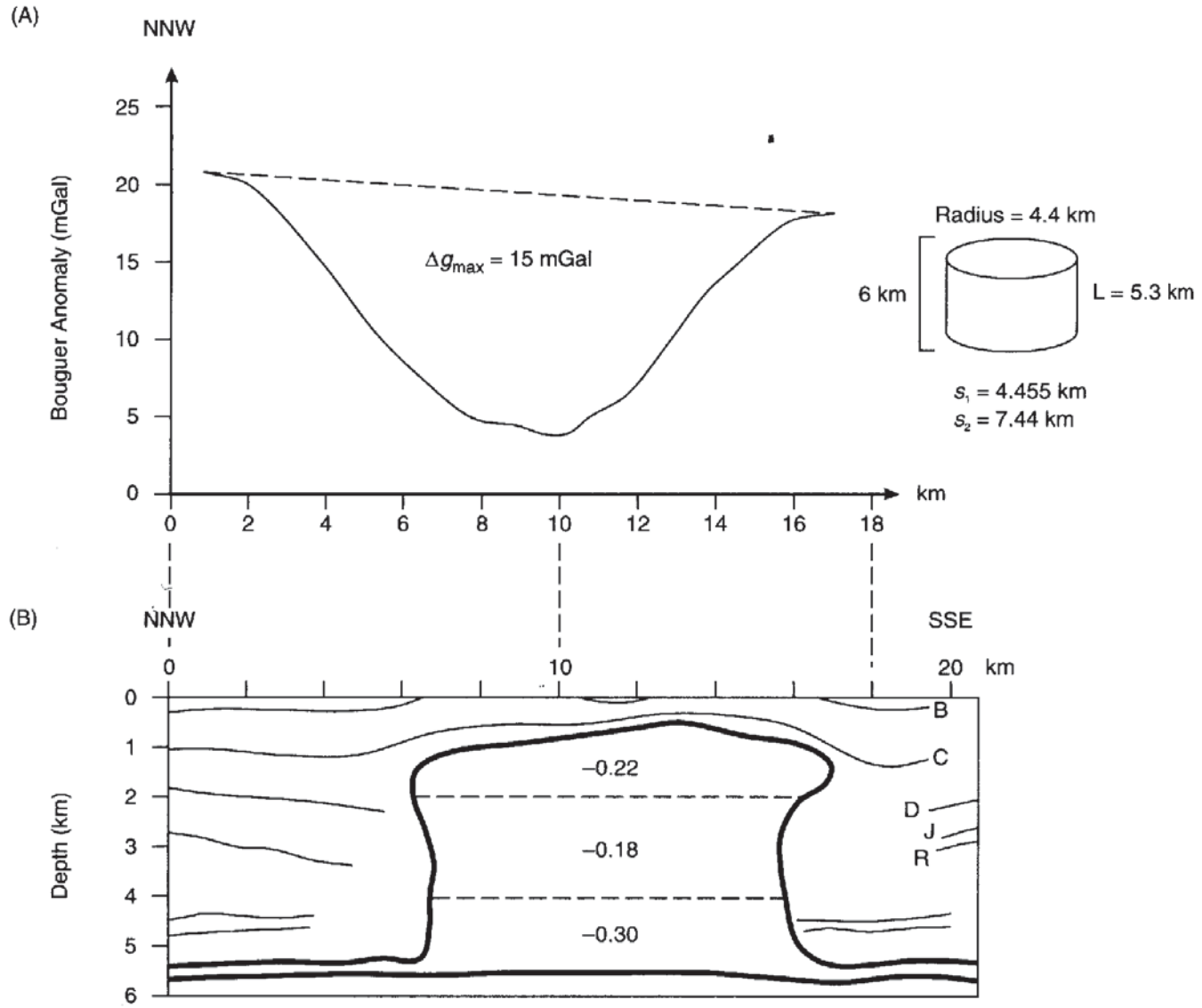

Figure 2.38 (A) Bouguer anomaly profile and (B) corresponding seismic section across profile A–B in Figure 2.37. After Kreitz (1982), LaFehr (1982) and Sharma (1986), by permission

Uncertainty in the density contrast is the biggest problem in interpretation. Subsequent drilling into the salt dome and the use of the seismic profiles undertaken radially across the salt dome enabled the geological model to be enhanced. It was found that the density contrast within the salt dome could be divided into three sections with slightly different density contrasts (Figure 2.38B). The seismic sections did not give a very good image of the top of the salt dome, which is mushroom-shaped and so causes the slight discrepancies between the sphere and vertical cylinder approximations. The combined use of seismic data and gravity modelling has resulted in a much more realistic geological model.

However, it should always be remembered that any geophysical model is only a crude approximation of what can be a very complex geological structure. Consider how well (or otherwise) a vertical cylinder

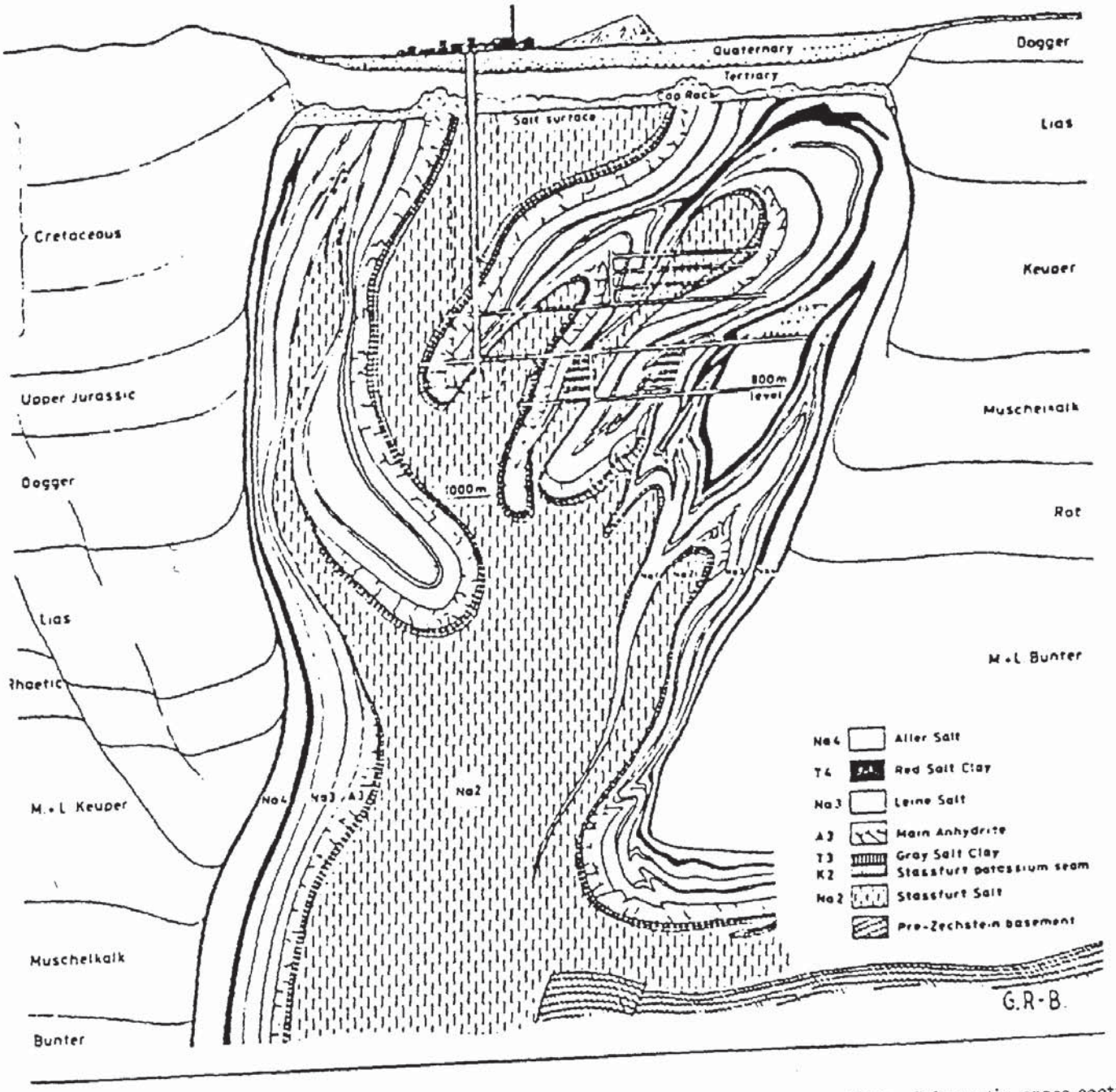

Figure 2.39 Schematic cross-section through a salt dome structure in north-west Germany, illustrating known complexities in contrast to the usual assumed geophysical model of a vertical cylinder with a uniform density distribution. From Sorgenfrei (1971) and Richter-Bernburg (1982), by permission

model would represent the salt dome illustrated in Figure 2.39. It is clear that much fine geological detail would not be resolvable unambiguously by the interpretation of geophysical data (Sorgenfrei 1971; Richter-Bernburg 1982).

2.7.1.2 Salt domes in NW Germany (hydrocarbons)

Another example of gravity anomalies over salt domes is given in Figure 2.40, which is taken from part of a survey over north-west Germany (Hermes, 1986). The intention was to derive the gravity field

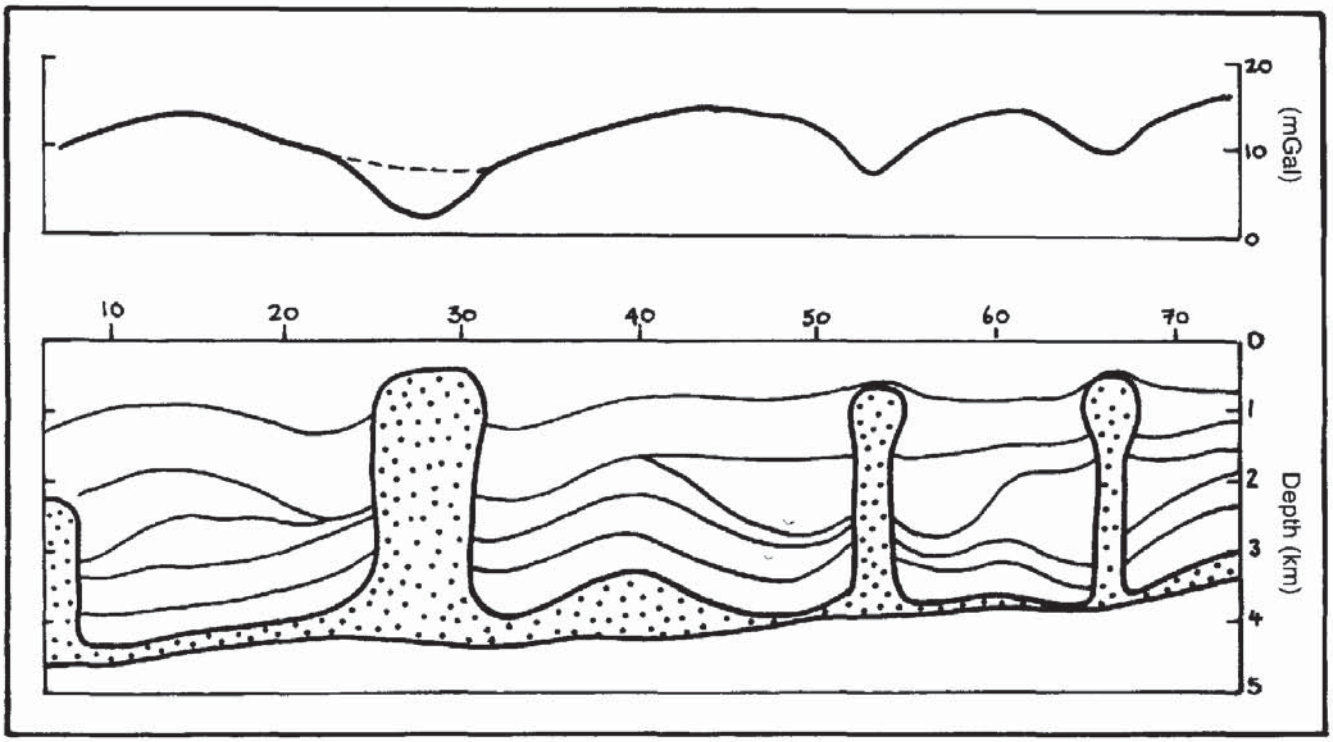

Figure 2.40 A typical Bouguer anomaly profile compared with the corresponding sub-surface geology associated with the Zechstein in northern Germany. From Hermes (1986), by permission

due to the pre-Zechstein and remove it, akin to gravity stripping, to be able to investigate what lies beneath it. Seismic reflection profiling has been singularly unsuccessful both in penetrating through this layer and in producing much useful information. The amplitudes of the Bouguer anomaly minima are clearly associated with the size of the salt domes, the smallest having the lowest amplitude (≈ 5 mGal). The largest minimum is a compound anomaly comprising a minimum associated with the syncline through which the low-density salt has risen. This emphasises the fact that the Bouguer anomaly map of this area is strongly influenced by the structures within the post-Zechstein and by the salt domes and walls. To determine the gravity effect of the pre-Zechstein it is thus essential that these effects be removed. Gravity stripping appears to succeed where filtering methods have been less successful.

2.7.2 Mineral exploration

Gravity surveys fulfil two roles in exploration for minerals: (1) for search and discovery of the ore body, and (2) as a secondary tool to delimit the ore body and to determine the tonnage of ore.

2.7.2.1 Discovery of the Faro lead–zinc deposit, Yukon

An integrated airborne and land geophysical exploration programme, of which gravity surveying was an integral part, led to the discovery of

the Faro lead–zinc deposit in the Yukon, northern Canada (Brock 1973). Gravity was found to be the best geophysical method to delimit the ore body (Figure 2.41). It was also used to obtain an estimate of the tonnage (44.7 million tonnes), which compared very well with a tonnage proven by drilling of 46.7 million tonnes (Tanner and Gibb 1979). In contrast, vertical magnetic mapping provided an anomaly with too shallow gradients to be used, as Figure 2.41 shows.

2.7.2.2 Pyramid ore body, North West Territories

The Pyramid lead–zinc ore body, at Pine Point in the North West Territories, Canada, was discovered using the 'induced polarisation' (IP) method (Seigel *et al.* 1968). For further details of IP, see Chapter 9. Gravity was used to optimise development drilling since the gravity anomalies (Figure 2.42) correlated extremely well with the distribution of the mineralisation within the ore body. Additionally, the gravity data were used successfully to estimate total ore tonnage. Electrical resistivity (see Chapter 7) produced low-amplitude anomalies with a broad correlation with the position of the ore body, and a TURAM electromagnetic survey (see Chapters 10 and 11) was singularly unsuccessful and produced virtually no anomaly at all. The induced polarisation chargeability produced a spectacular anomaly.

2.7.2.3 Sourton Tors, Dartmoor, SW England

This is an example of where gravity did not work at all in association with a known occurrence of mineralisation (Figure 2.43), whereas electrical, electromagnetic and magnetic methods all produced significant anomalies (Beer and Fenning 1976; Reynolds 1988). The reason for the failure of the gravity method in this case is twofold:

- The scale of mineralisation, which is a stockwork of mineralised veins, was of the order of only a few metres wide.
- The sensitivity of the gravimeter was insufficient to resolve the small density contrast between the sulphide mineralisation and the surrounding rocks.

Had a gravimeter capable of measuring anomalies of the order of tens of μGal, and the station interval been small enough, then the zone of mineralisation may have been detectable. At the time of the survey (1969), such sensitive gravimeters were not as widely available as they are today.

2.7.3 Glacier thickness determination

For a regional gravity survey to be complete in areas such as Antarctica and Greenland, measurements have to be made over ice

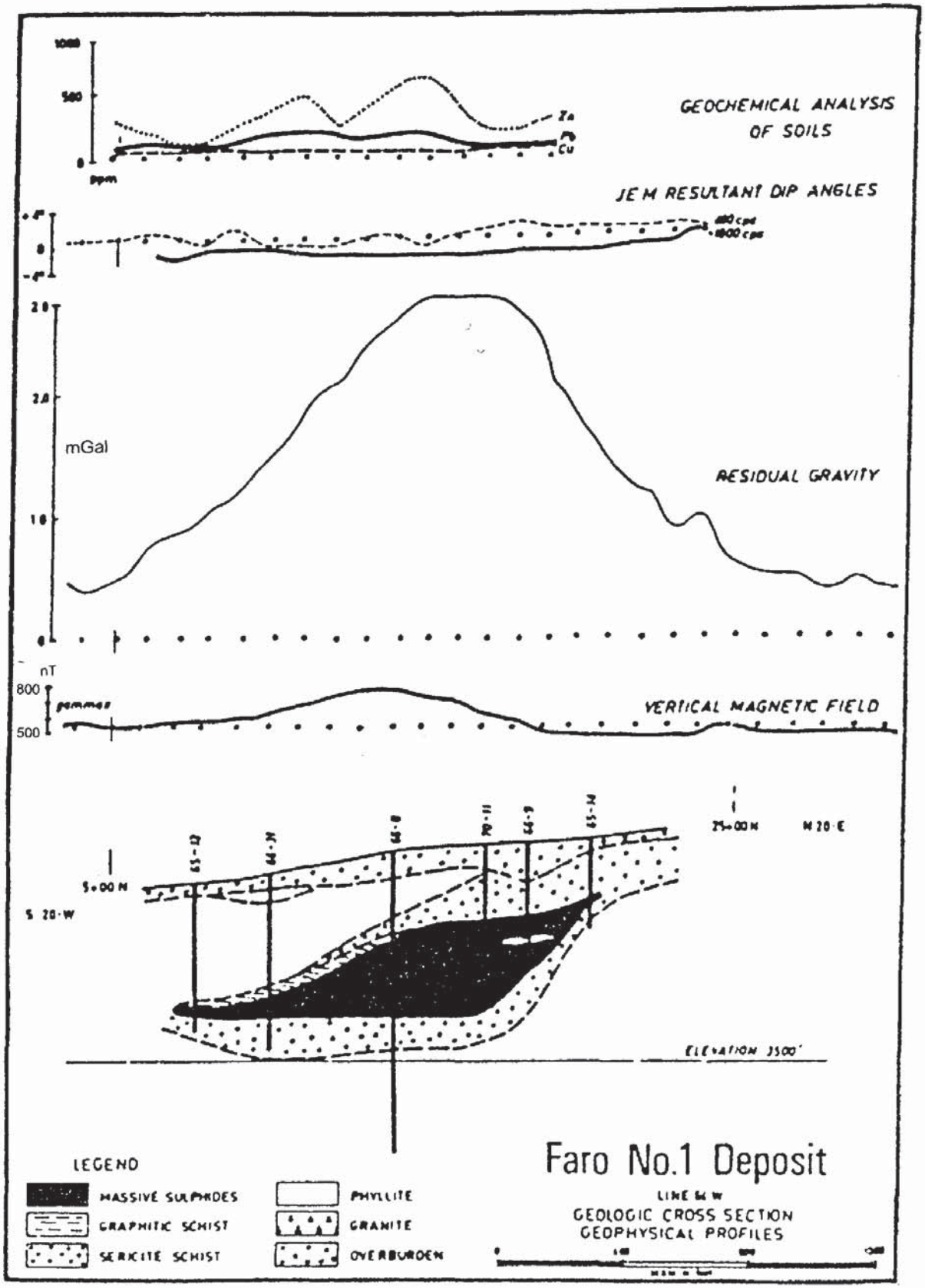
GEOCHEMICAL ANALYSIS OF SOILS
Zn
Cu
ppm
JEM RESULTANT DIP ANGLES
mGal
RESIDUAL GRAVITY
nT
VERTICAL MAGNETIC FIELD
S 20·W
N 20·E
ELEVATION 3500'
LEGEND
MASSIVE SULPHIDES
GRAPHITIC SCHIST
SERICITE SCHIST
PHYLLITE
GRANITE
OVERBURDEN
Faro No.1 Deposit
LINE 64 W
GEOLOGIC CROSS SECTION
GEOPHYSICAL PROFILES

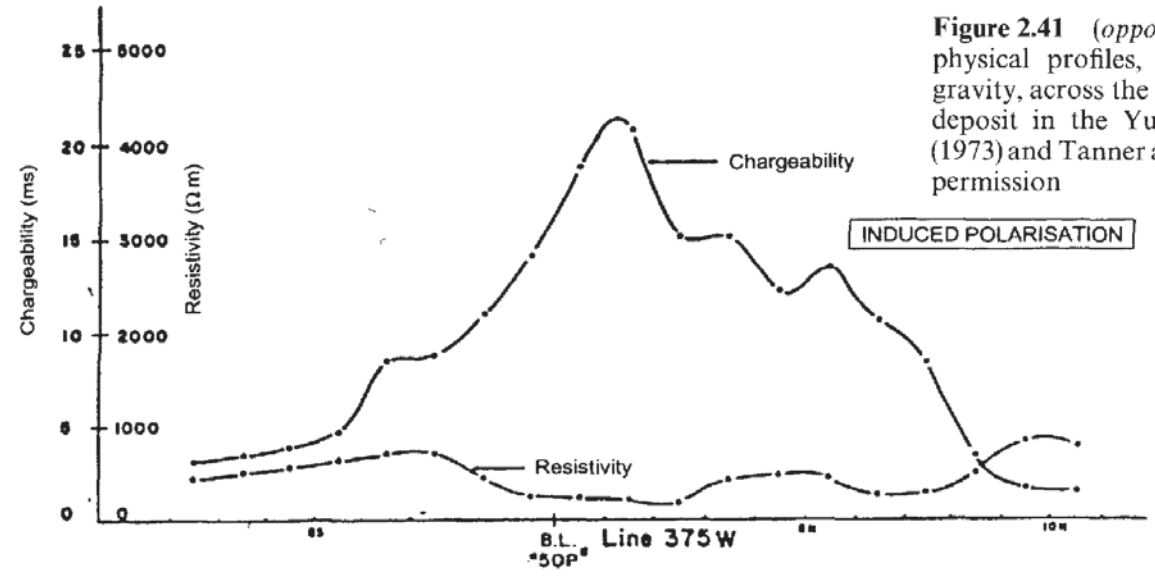

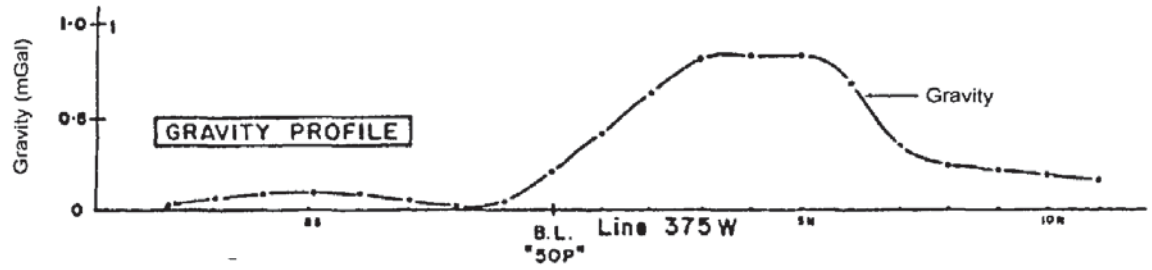

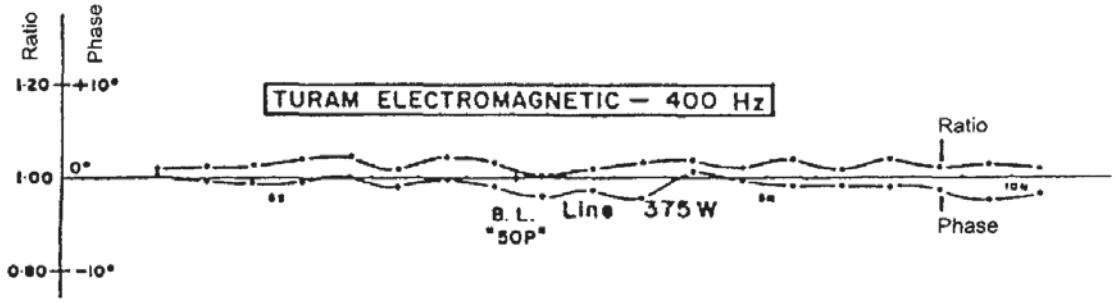

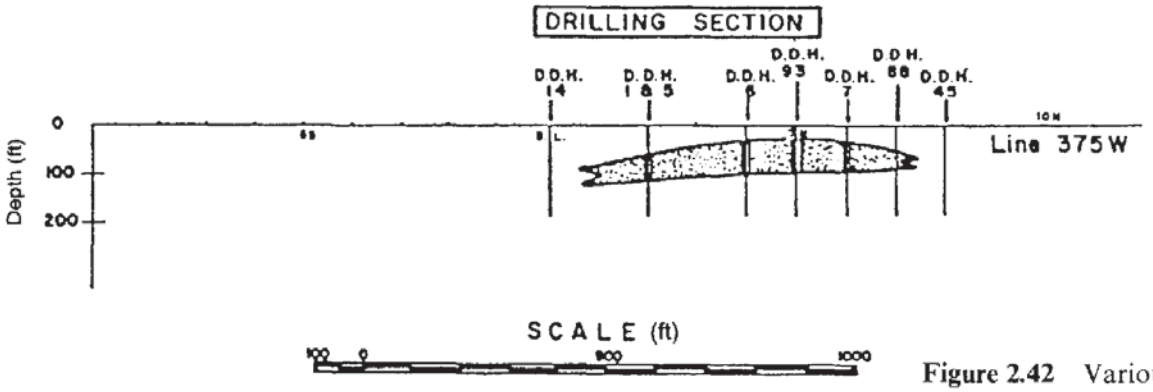

Figure 2.41 (*opposite*) Various geophysical profiles, including residual gravity, across the Faro lead–zinc ore deposit in the Yukon. From Brock (1973) and Tanner and Gibb (1979), by permission

Figure 2.42 Various geophysical profiles including residual gravity, across Pyramid no. 1 ore body. From Seigel *et al.* (1968), by permission

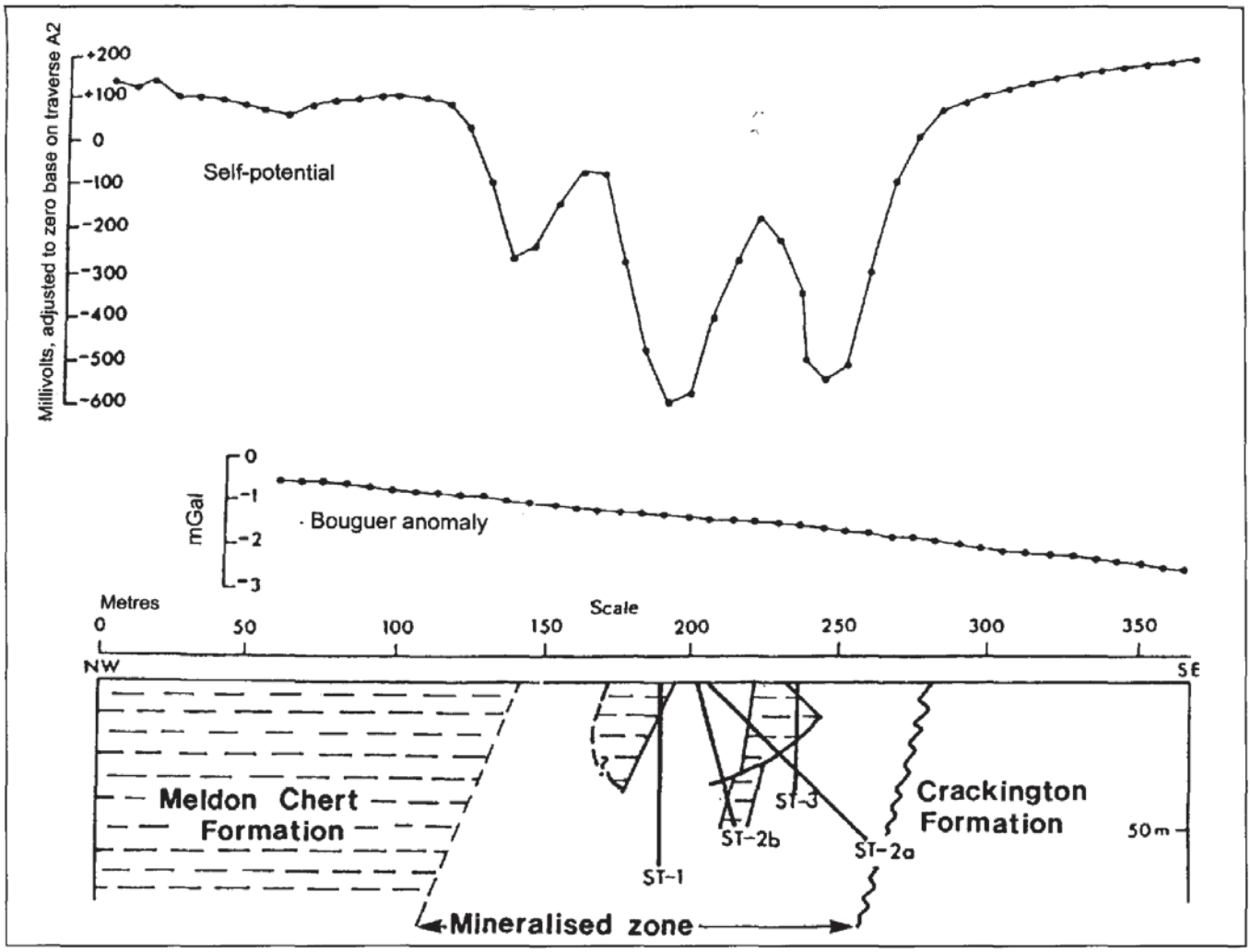

Figure 2.43 A Bouguer gravity profile across mineralised zones in chert at Sourton Tors, north-west Dartmoor, showing no discernible anomalies. From Beer and Fenning (1976), by permission

sheets and valley glaciers. Very often, these areas have incomplete information about the depth or volume of ice. The large density difference between ice (0.92 Mg/m^3) and the assumed average rock density (2.67 Mg/m^3) means that easily measured gravity anomalies can be observed and the bottom profile of the ice mass (i.e. the sub-glacial topography) can be computed.

An example of this has been given by Grant and West (1965) for the Salmon Glacier in British Columbia (Figure 2.44), in which a gravity survey was undertaken in order to ascertain the glacier's basal profile prior to excavating a road tunnel beneath it. A residual gravity anomaly minimum of almost 40 mGal was observed across the glacier, within an accuracy of ± 2 mGal due to only rough estimates having been made for the terrain correction. An initial estimate of local rock densities was 2.6 Mg/m^3 and the resultant depth profile across the glacier proved to be about 10% too deep (Figure 2.44B) compared with depths obtained by drilling. Considering the approxi-

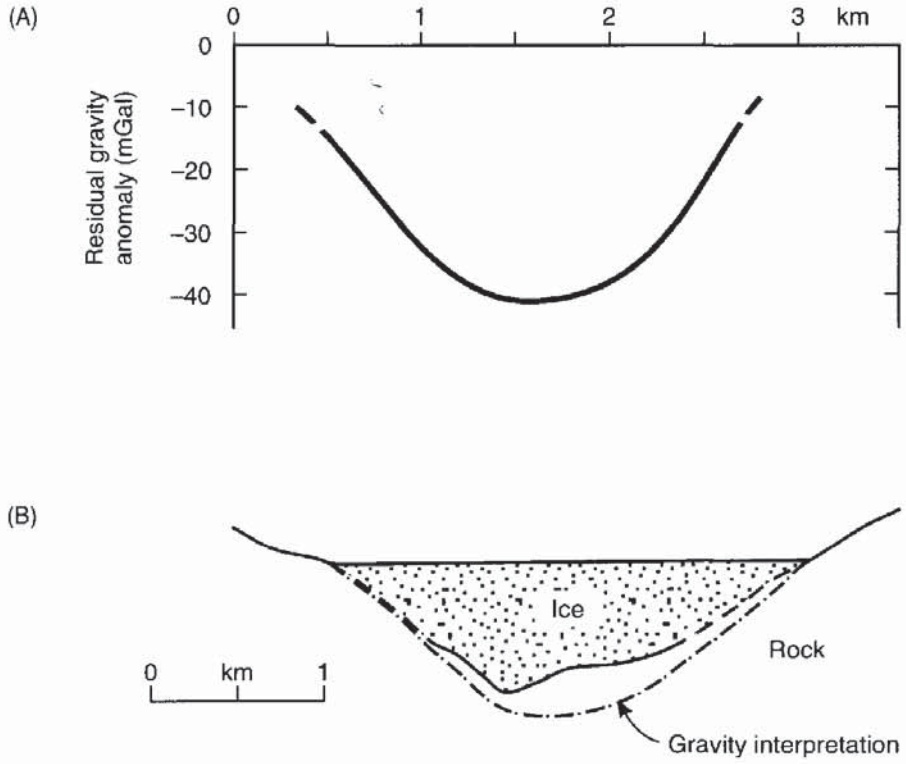

Figure 2.44 A residual gravity profile across Salmon Glacier, British Columbia, with the resulting ice thickness profile compared with that known from drilling. After Grant and West (1965), by permission

mations taken in the calculations, the agreement was considered to be fair. In addition, it was found that the average density of the adjacent rocks was slightly lower (2.55 Mg/m^3). This could have indicated that there was a significant thickness of low-density glacial sediments between the sole of the glacier and bedrock. However, had more detailed modelling been undertaken on data corrected fully for terrain, the discrepancy could have been reduced.

Increasingly, ice thickness measurements are being made by seismic reflection surveying (see Chapter 5), electromagnetic VLF measurements (see Chapter 9, Section 9.6.6.3) and radio echosounding (see Chapter 9, Section 9.7.4.2). Comparisons between the various geophysical methods indicate that agreements of ice thickness within 10% can be readily obtained. Gravity measurements over large ice sheets (e.g. Renner *et al.* 1985; Herrod and Garrett 1986) can be considerably less accurate than standard surveys for three reasons:

- The largest errors are due to the imprecise determination of surface elevations. Currently, heights can be determined to within 5–10 m.
- Inaccurate corrections for sub-ice topography vary by hundreds of metres, in areas without radio echosounding control. An error in estimated ice thickness/bedrock depth of 100 m can introduce an error of ± 74 g.u.
- As in all gravity surveys, the estimate of the Bouguer correction density is also of critical importance. Major ice sheets obscure the

local rock in all but a few locations, and the sub-ice geology, and its associated densities, may vary significantly.

Another glaciological application of the gravity method is the use of a gravimeter to measure oceanic tidal oscillations by the vertical movements of floating ice shelves in the Antarctic (Thiel *et al.* 1960; Stephenson 1984). The resulting tidal oscillation pattern can be analysed into the various tidal components and hence relate the mechanical behaviour of the ice shelf to ocean/tidal processes. If tidal oscillations are not found at particular locations, this may indicate that the ice shelf is grounded. Independent measurements with tilt meters, strain gauges and radio echosounding should be used to confirm such a conclusion (Stephenson and Doake 1982).

2.7.4 Engineering applications

The size of engineering site investigations is normally such that very shallow (< 50 m) or small-scale (hundreds of square metres) geological problems are being targeted. Consequently, the resolution required for gravity measurements is of the order of μGals. The use of gravity is commonly to determine the extent of disturbed ground where other geophysical methods would fail to work because of particularly high levels of electrical or acoustic noise, or because of the presence of a large number of underground public utilities (Kick 1985). Additionally, gravity is used to assess the volume of anomalous ground, such as the size of underground cavities or of ice lenses in permafrost. There are often no records of where ancient quarrying or mining has been undertaken and the consequent voids may pose considerable hazards to people and to property. The increasing development of higher latitudes brings its own engineering problems, and the application of gravity surveying, amongst other applied geophysical methods, is playing a growing and important role in site investigations in these areas. Furthermore, it is also true to say that with the increased use of geophysical methods, the very geological phenomena under investigation are becoming better studied and better known.

2.7.4.1 Detection of back-filled quarries

Where there is sufficient density contrast between infill material and the surrounding rock, small-scale gravity surveys can be used successfully to locate backfilled quarries (Poster and Cope 1975), as the following example demonstrates.

A proposed new railway section in Newcastle-upon-Tyne, England, was routed through a built-up area which contained a number of backfilled, late-nineteenth century sandstone quarries. The design of the section of railway included a cut-and-cover tunnel, and so it was

extremely important to determine the position of the old quarry faces very accurately. The nature of the loose infill material (density 1.65 M/m^3) provided a strong contrast in physical properties with the local sandstone (of density 2.1 Mg/m^3) and a number of geophysical methods could have been employed. However, the site was criss-crossed by a large number of underground pipes and cables, and the superficial material contained significant amounts of scrap metal, all of which made it impractical to use electrical, electromagnetic or magnetic methods. High levels of acoustic noise which were generated by large volumes of traffic during the working day, and the lack of space due to extensive building cover, precluded the use of seismic methods. Consequently, the gravity method was selected and operated between the hours of midnight to 6 a.m., thus avoiding the problems of vibrations arising from both traffic and from heavy industrial plant, and ensuring better access through the reduction in the number of parked cars.

The contrast in density between the infill material and the local sandstone (0.5 Mg/m^3) produced small but detectable residual gravity anomalies of the order of 0.7 mGal. The gravity data were reduced and interpreted with the aid of data from one borehole and a preliminary archaeological investigation. A map of the residual gravity anomalies (Figure 2.45) clearly illustrates the locations of the faces of two quarries.

2.7.4.2 Detection of massive ice in permafrost terrain

The thawing of massive ice masses and associated ice-rich permafrost can cause severe engineering and environmental problems. The detection and identification of such ground phenomena is thus extremely important.

Kawasaki *et al.* (1983) provide an example of the use of gravity surveying to detect the presence and the volume of massive ice within an area of permafrost at Engineer Creek, near Fairbanks, Alaska, along the route of a proposed road cut. It is well known that large bodies of massive ice, such as occur within pingos, give rise to significant gravity anomalies (Mackay 1962; Rampton and Walcott 1974). Permafrost without discrete segregated ice has a density of about 1.6 Mg/m^3, compared with the density of solid ice (0.88–0.9 Mg/m^3) and with that of typical Alaskan soils (1.35–1.70 Mg/m^3) and should give rise to detectable residual gravity anomalies if measured with a sufficiently sensitive gravimeter.

Kawasaki and colleagues demonstrated that, although massive ice can be detected by correlation with the gravity minima along the profile shown in Figure 2.46, the measurements were also sensitive to variations of density within the schist bedrock.

The gravity method is considered an excellent tool for detailed investigation of construction sites where massive ice is suspected, but

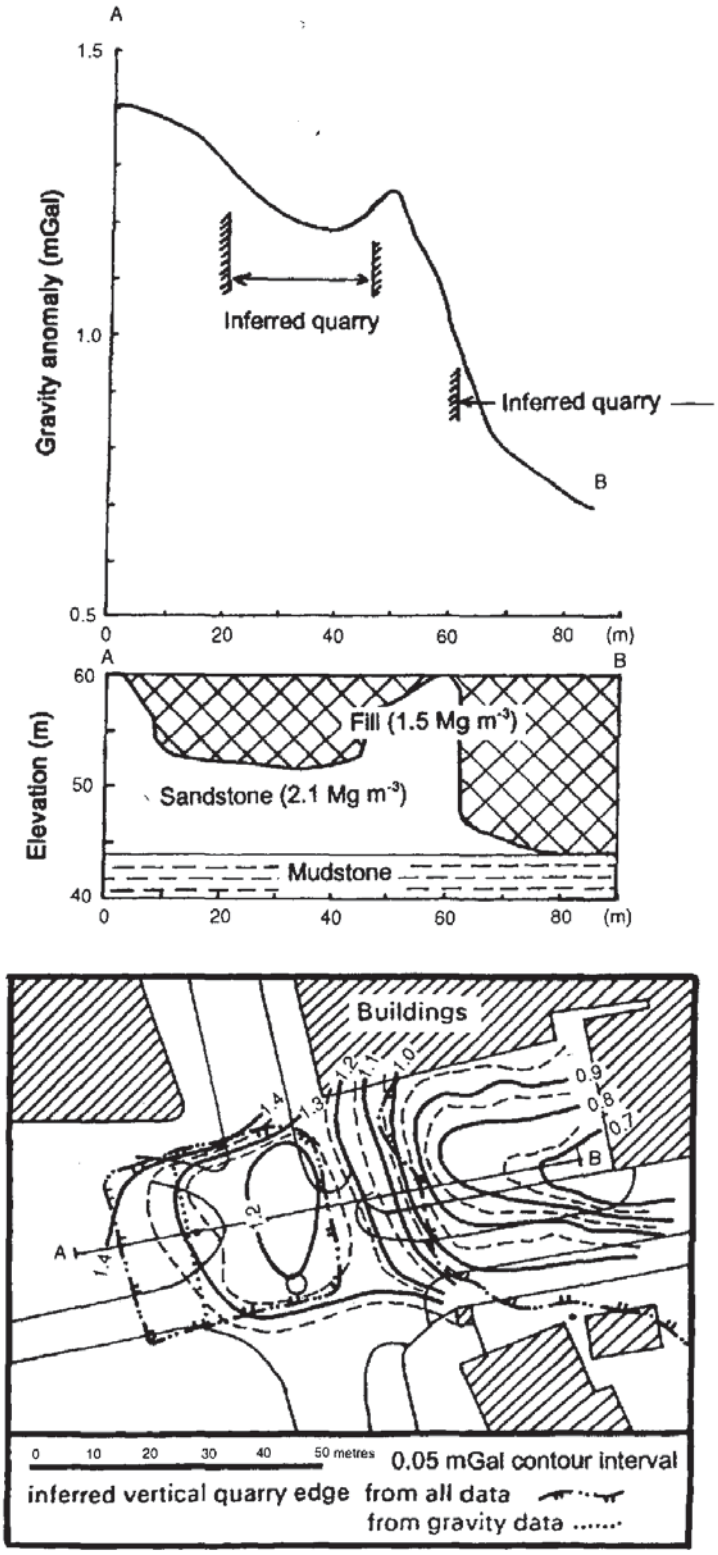

Figure 2.45 The top shows a residual gravity profile across infilled sandstone quarries in Newcastle-upon-Tyne. The cross-section and plan are also shown. After Poster and Cope (1975), by permission

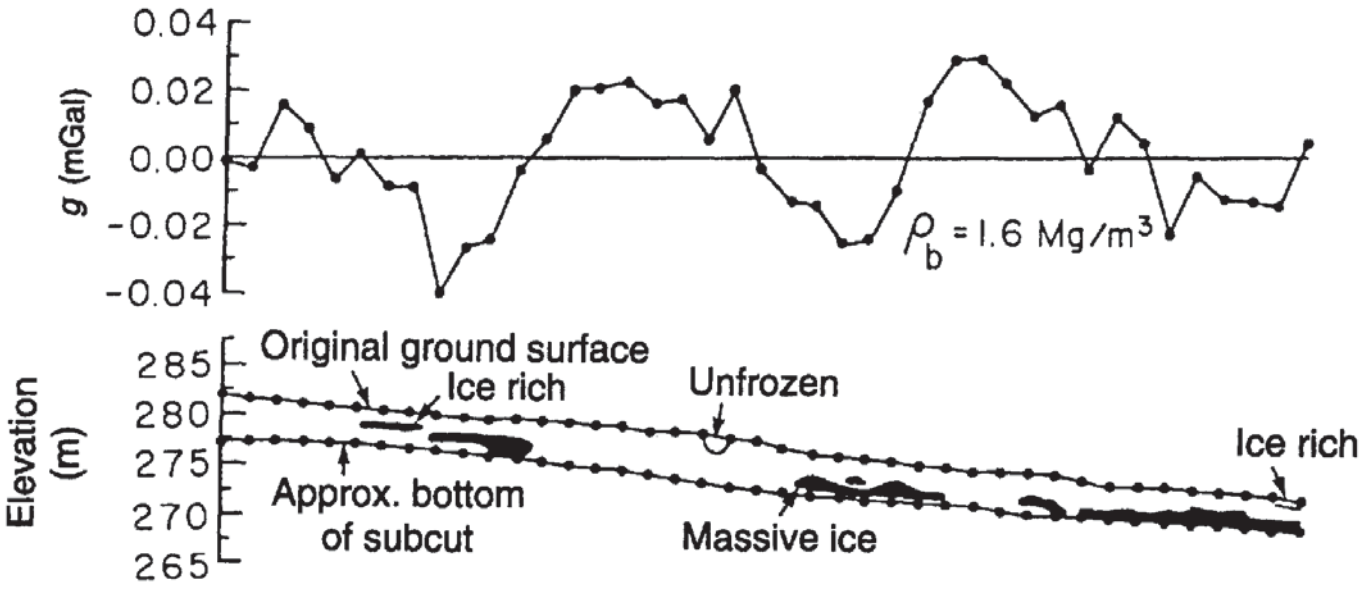

Figure 2.46 Gravity profile across massive ground ice in a road cut at Engineer Creek, near Fairbanks, Alaska. After Kawasaki *et al.* (1983), by permission

it is too slow a method for use as a reconnaissance tool over long profiles. Other geophysical methods such as electrical resistivity, electromagnetic ground conductivity and ground-penetrating radar are more efficient, particularly for reconnaissance (Osterkamp and Jurick 1980).

2.7.5 Detection of underground cavities

Hidden voids within the near-surface can become serious hazards if exposed unwittingly during excavation work, or if they become obvious by subsidence of the overlying ground (Figure 2.47). The detection of suspected cavities using gravity methods has been achieved in many engineering and hydrogeological surveys (e.g. Colley 1963). Gravimetry is increasingly of interest to archaeologists searching, for example, for ancient crypts or passages within Egyptian pyramids, such as has been achieved within the Kheops (see *First Break*, 1987 5(1): 3) with what is called 'endoscopic micro-gravity' (see also Lakshmanan 1991).

2.7.5.1 Hidden natural cavities

An example of the application of micro-gravimetry to the detection of underground cavities has been given by Fajklewicz (1986). Over many years he has investigated the gravity effect of both natural and man-made cavities and has helped to develop a method of detection based on calculating the vertical gradient of the gravity field. He has found that the amplitude of the gravity anomaly is commonly greater than that predicted (Figure 2.48) for reasons that are still not clear.

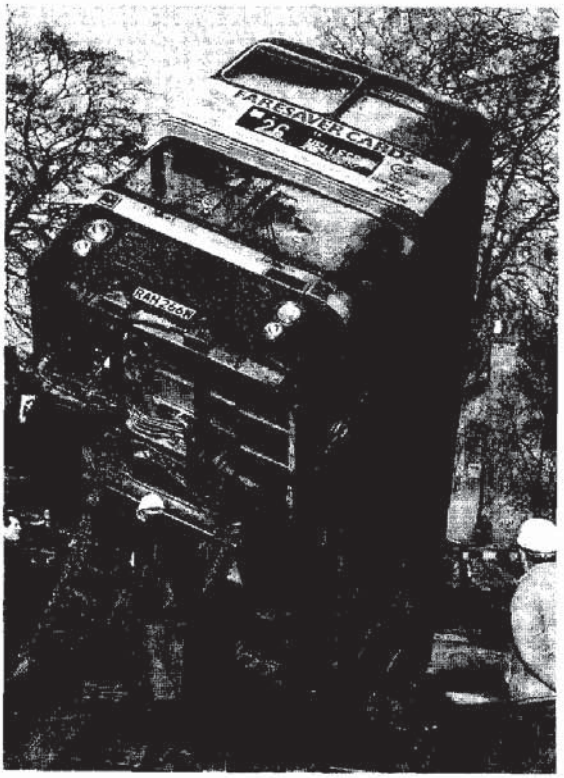

Figure 2.47 Catastrophic failure of the roof of an ancient flint mine in chalk in Norwich. Photo courtesy of Eastern Daily Press

A micro-gravity survey was carried out in the town of Inowrocław, Poland, where karst caverns occur to depths of around 40 m in gypsum, anhydrite, limestone and dolomite. The cavities develop towards the ground surface and have resulted in the damage and destruction of at least 40 buildings within the town. The density contrast between the cavity and the surrounding material in Figure 2.48A is $-1.8\ \mathrm{Mg/m^3}$ and for Figure 2.48B is $-1.0\ \mathrm{Mg/m^3}$, slightly lower due to the presence of rock breccia within the cavity. Fajklewicj has demonstrated that the cavity in Figure 2.48B should not have been detectable assuming that its gravity field is due entirely to a spherical cavity at the depth shown. Even the theoretical anomaly from the vertical gravity gradient is too broad to indicate the presence of a cavity, yet the observed anomaly is quite marked.

A similar approach can be taken using horizontal gravity gradients ($\Delta g/\Delta x$ or $\Delta g/\Delta y$), in which case the point at which the gravity anomaly reaches a minimum or maximum, the gradient goes through zero, and that point should lie over the centre of the body causing the anomaly (Butler 1984). An example of this (Figure 2.49) is given by Casten and Gram (1989) for a test case where gravity data were measured in a deep coal mine along an inclined drift which was known to pass at right-angles over a pump room.

Furthermore, micro-gravimetry can be used to determine the rate and extent of the development of strength-relaxation around underground excavations, as shown in Figure 2.50 (Fajklewicz 1986;

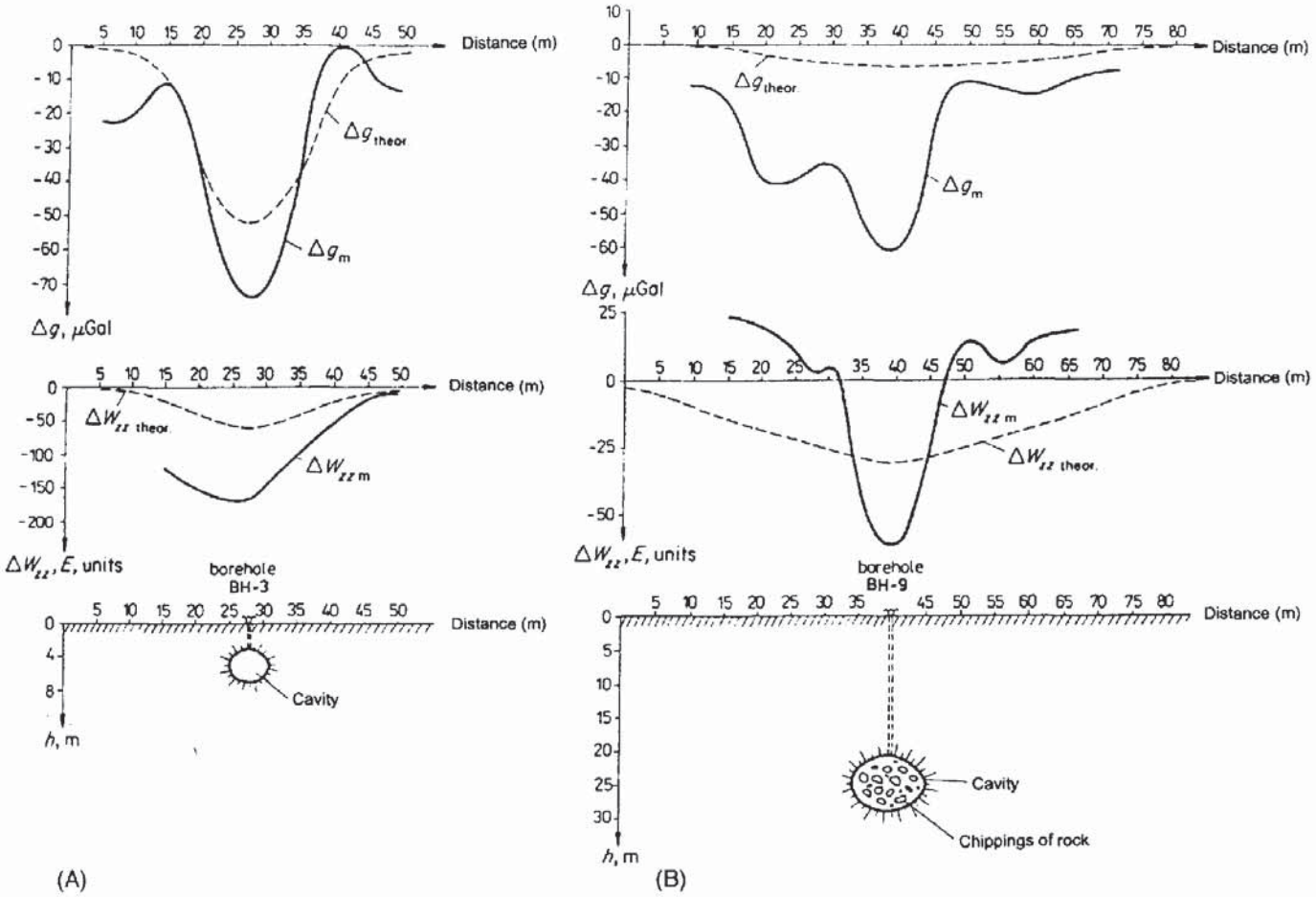

Figure 2.48 Δg_m and $\Delta W_{zz.m}$ micro-gravity anomalies and gravity gradient anomalies respectively–over (A) an air-filled cavity (BH-3), and (B) one partially infilled by rock fragments (BH-9). Curves labelled with suffix 'theor' represent the theoretical anomalies based on the parameters of the cavity alone. From Fajklewicz (1986), by permission

Gluśko *et al.* 1981). As the rock relaxes mechanically it cracks, thereby reducing its bulk density. As the cracking continues and develops, so the changes in density as a function of time can be detected using highly sensitive micro-gravimeters, and then modelled.

2.7.5.2 *Archaeological investigations*

Blizkovsky (1979) provides an example of how a careful micro-gravity survey revealed the presence of a suspected crypt within the St 'Venceslas church, Tovacov, Czechoslovakia, which was later proven by excavation work. The dataset consisted of 262 values measured on a $1\,m^2$ or $4\,m^2$ grid to an accuracy of $\pm 11\,\mu$Gal, corrected for the gravity effect of the walls of the building (Figure 2.51). Two significant gravity minima with relative amplitudes of $-60\,\mu$Gal were located which indicated mass deficiencies associated with the previously unknown crypts.

2.7.6 Hydrogeological applications

Gravity methods are not used as much as electrical methods in hydrogeology but can still play an important role (Carmichael

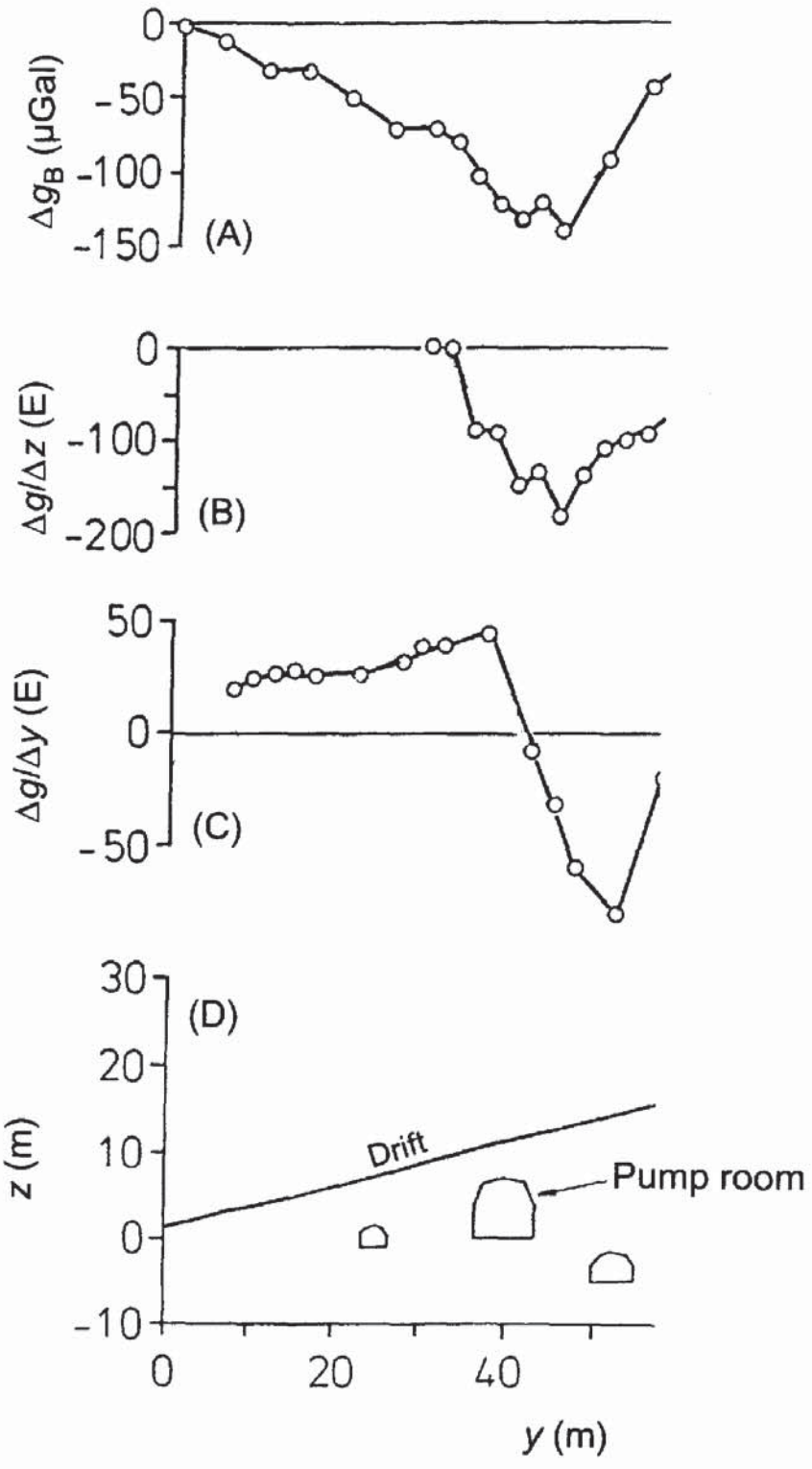

Figure 2.49 A micro-gravity survey within a deep coal mine as measured along a drift cut over a pump room and other known cavities. (A) shows observed residual gravity profiles; (B) observed and computed vertical gravity gradients; (C) observed horizontal gravity gradient, and (D) underground positions of known cavities from mine plans. From Casten and Gram (1989), by permission

and Henry 1977). Their more normal use is to detect low-density rocks that are thought to be suitable aquifers, such as alluvium in buried rock valleys (Lennox and Carlson 1967; van Overmeeren 1980).

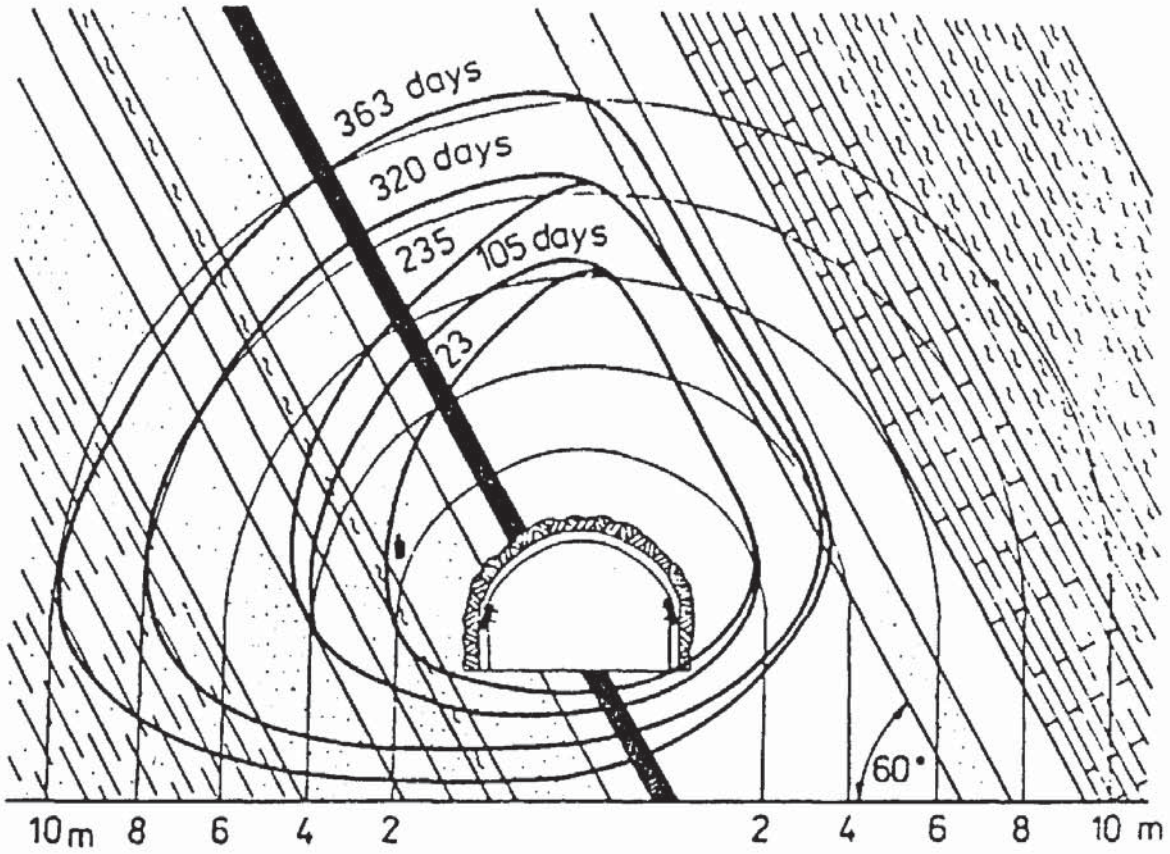

Figure 2.50 The time-dependent strength-relaxation around an underground gallery at 540 m depth as deduced from micro-gravity surveying in the Tchesnokov Colliery in the Don Basin over a period of 363 days. From Gluśko *et al.* (1981) and Fajklewicz (1986), by permission

Buried valleys, which have been incised into either bedrock or glacial till and are associated with the South Saskatchewan River, have been identified by their gravity effects (Hall and Hajnal 1962). The Bouguer anomaly across the current river valley shows a minimum considerably wider than the present-day valley (Figure 2.52), thus indicating the presence of low-density material – subsequently found by drilling to be silts and sand.

Rather than interpret Bouguer anomalies, it is possible to use a gravimeter to monitor the effect of changing groundwater levels. For example, in a rock with a porosity of 33% and a specific retention of 20%, a change in groundwater level of 30 m could produce a change in g of 170 μGal. It is possible, therefore, to use a gravimeter to monitor very small changes in g at a given location. The only changes in gravity after corrections for instrument drift and Earth tides should be the amount of water in the interstices of the rock. Consequently, for an aquifer of known shape, a measured change in gravity, in conjunction with a limited number of water-level observations at a small number of wells, can be translated into an estimate of the aquifer's specific yield. Similarly, repeated gravity measurements have been used to estimate the volume of drawdown, degree of saturation of the steam zone (Allis and Hunt 1986) and the volume of

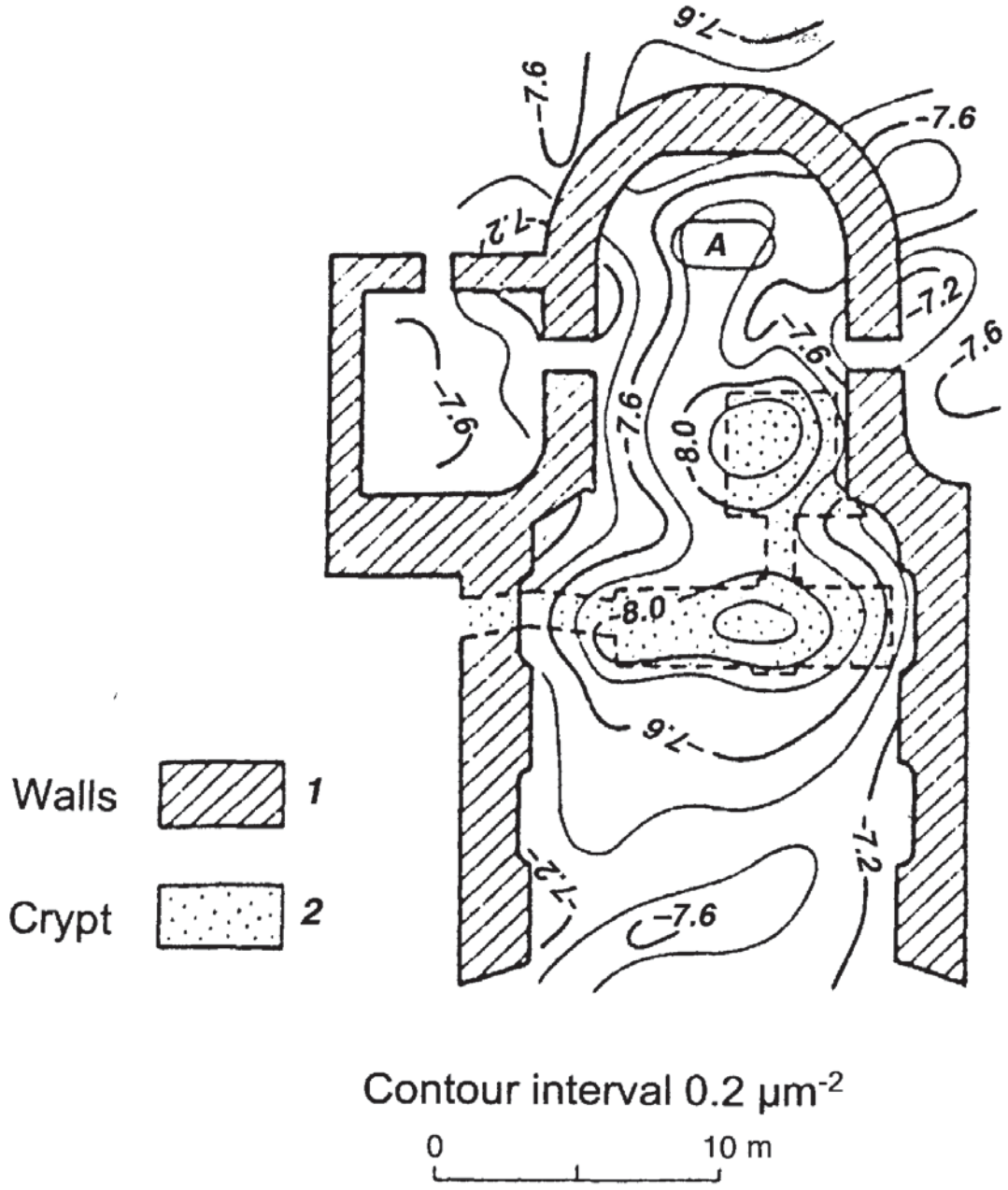

recharge of the Wairakei geothermal field, North Island, New Zealand (Hunt 1977).

Figure 2.51 Micro-gravity map of St 'Vencеslas Church, Tovacov, Czechoslovakia showing marked anomalies over previously unknown crypts. From Blizkovskt (1979), by permission

2.7.7 Volcanic hazards

With the advent of highly accurate surveying equipment and methods, and the availability of very sensitive gravimeters, it is possible to monitor small changes in the elevations of the flanks of active volcanoes – ultimately with a view to predicting the next eruption. Such studies are often accompanied by seismic monitoring

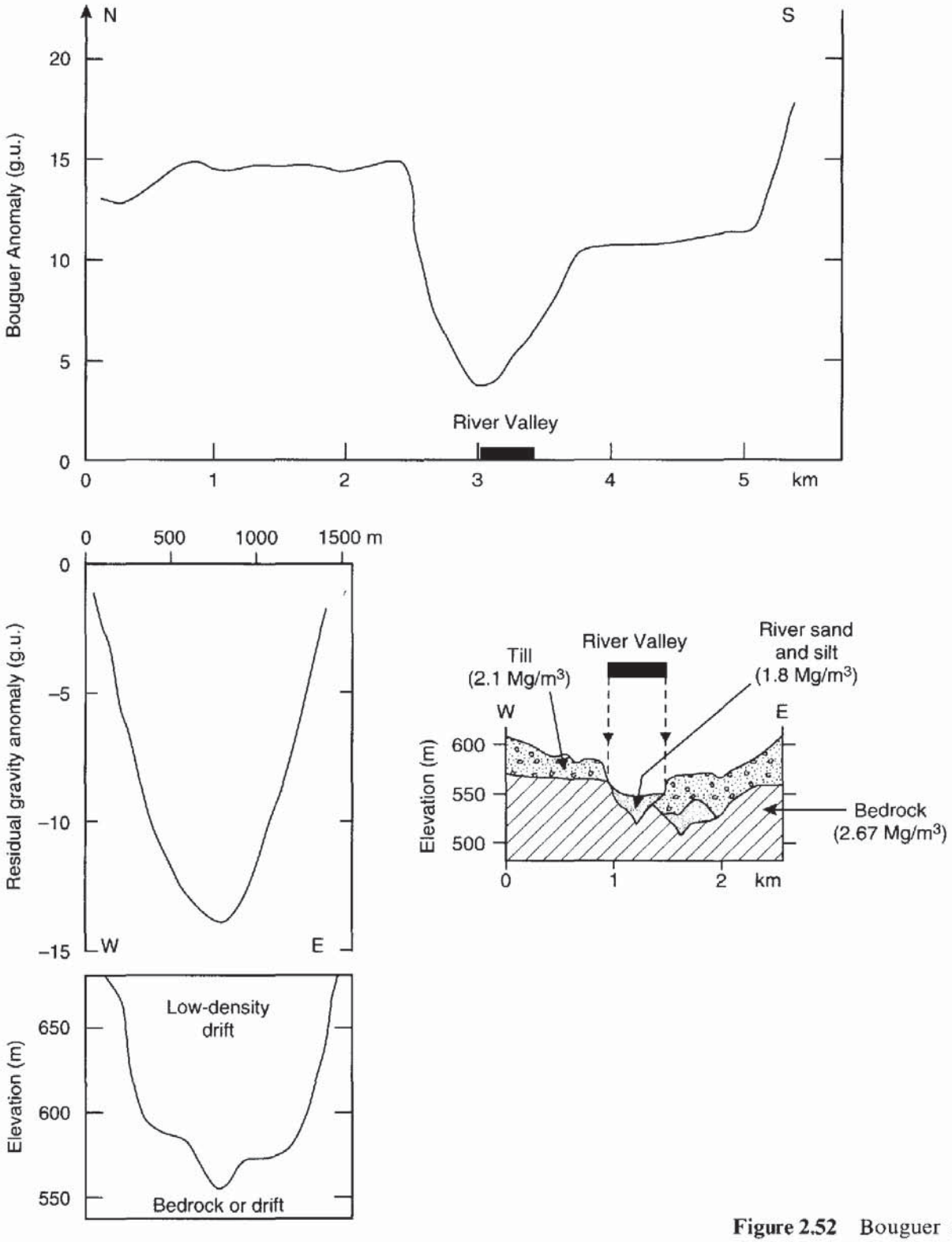

Figure 2.52 Bouguer anomaly over the South Saskatchewan River Valley, and the corresponding geological cross-section across the gravity minimum. After Hall and Hajnal (1962), by permission

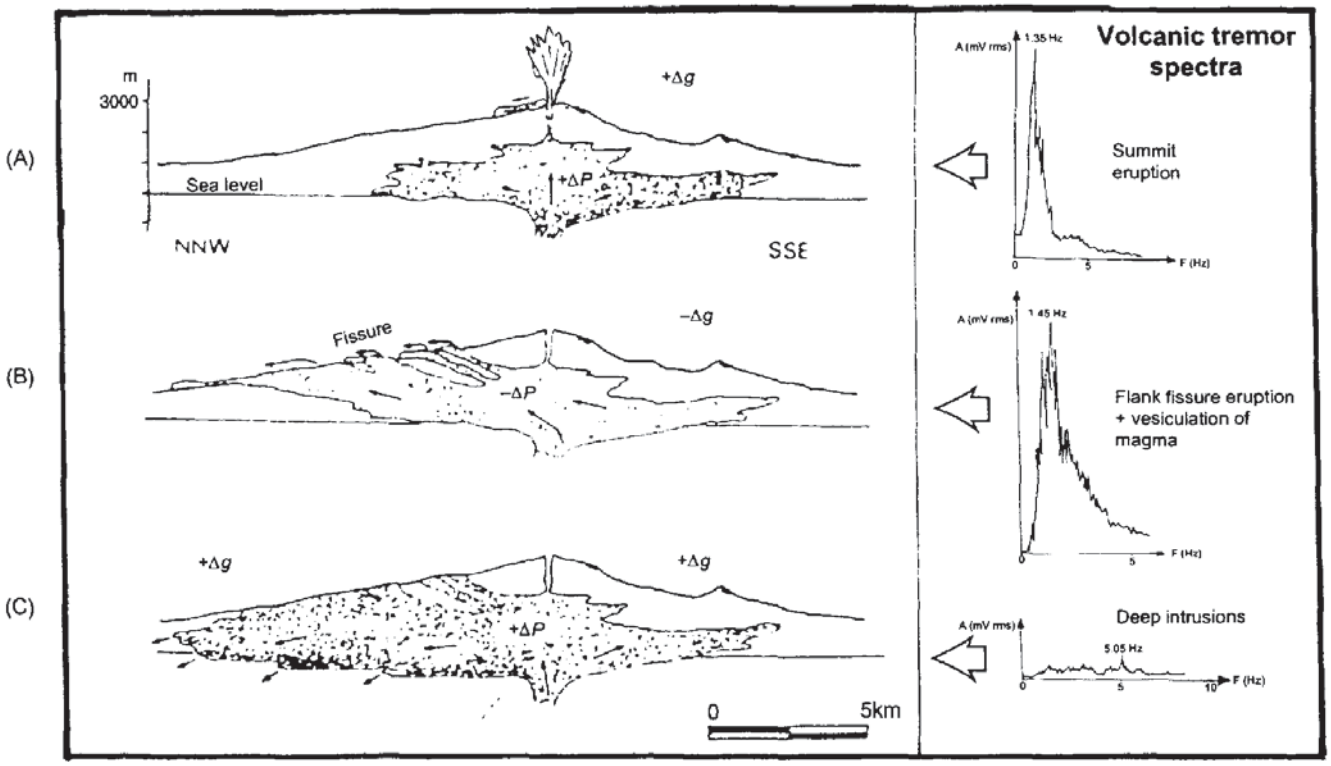

Figure 2.53 Sketches of the stages of fissure eruptions on Mt Etna, Sicily, with gravity trends and typical volcanic tremor spectra. From Sanderson *et al.* (1983) and Cosentino *et al.* (1989), by permission

(e.g. Cosentino *et al.* (1989). Sanderson *et al.* (1983) carried out such a gravity monitoring and levelling programme on Mount Etna, Sicily, during the period August 1980 to August 1981, during which time a flank eruption took place (17–23 March 1981) from which a lava flow resulted which narrowly missed the town of Randazzo. A series of schematic diagrams is shown in Figure 2.53 to illustrate the three clear stages of the fissure eruption.

Changes in gravity in association with elevation increases were interpreted as the injection of new magma at depth during the intrusion of a new dyke at about 1.5 km depth (Figure 2.53A). Gravity decreases were observed when eruptions took place because of the reduction in material (Figure 2.53B). Where increases in gravity were observed without an increase in elevation, this was interpreted as being due to the density of the magma increasing by the enforced emplacement of new material at depth (Figure 2.53C). The magnitude of the gravity changes (≈ 2–$25\,\mu$Gal) coupled with the known variations in elevation ($< \approx 20$ cm) provide a means of determining where within the volcano's plumbing the intrusions of new material and/or density changes are taking place.

Rymer and Brown (1987, 1989) have summarised the micro-gravity effects resulting from vertical movements of the magma/rock interface, vesiculation cycles with the magma column and radial changes in the dimensions of the magma body for Poás volcano in Costa Rica

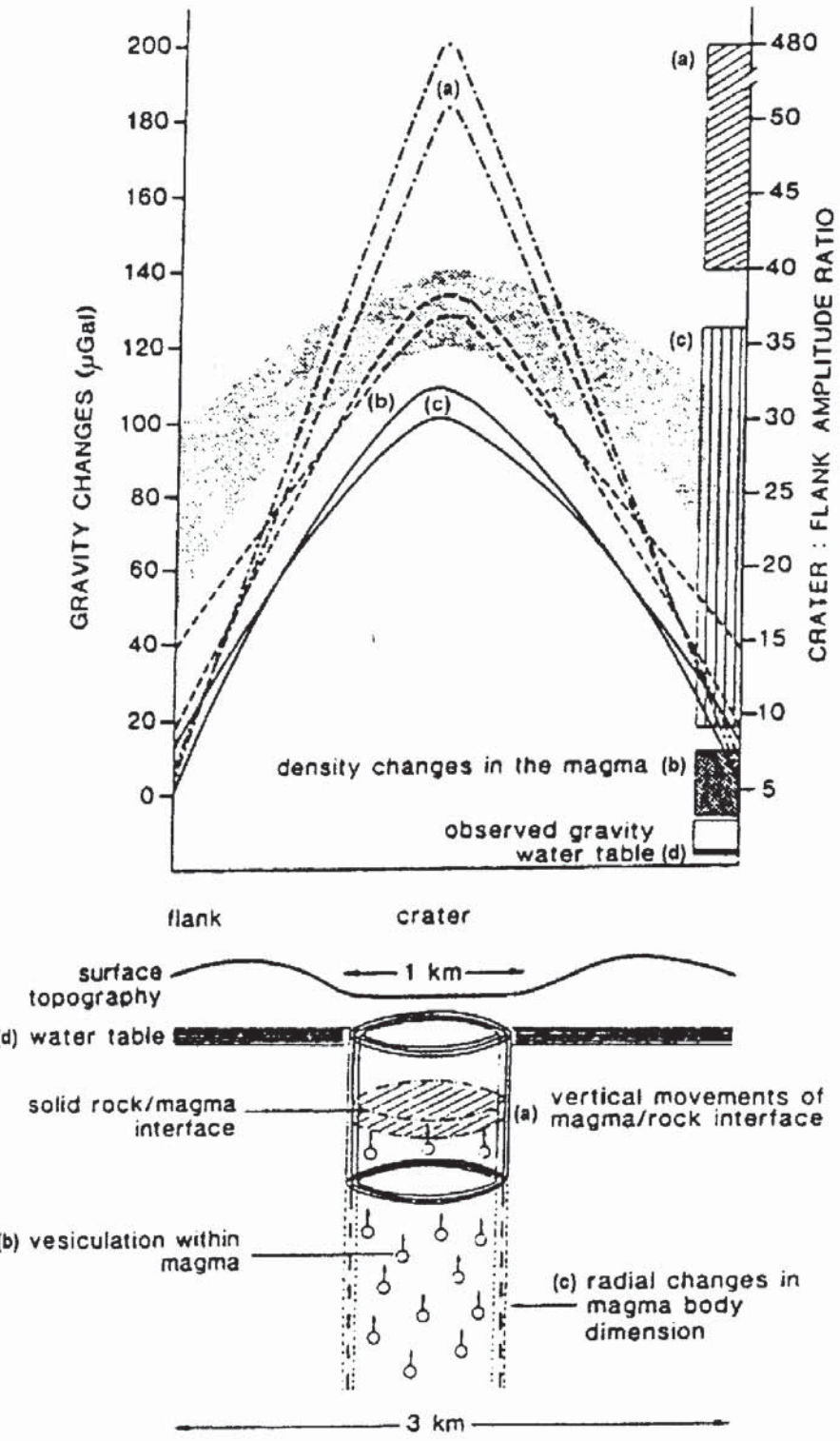

Figure 2.54 The top shows a schematic of the various gravity effects produced at the flank and summit of Poás volcano, Costa Rica (the observed range of gravity effects is shaded) and the ratio of the two (shown alongside in the vertical bar) as caused by different geological processes within the volcano (lower diagram). The processes are: (a) vertical movements of the magma/rock interface; (b) vesiculation cycles within the magma column; (c) radial changes in dimension of the magma column, and (d) variations in the level of the water table. From Rymer and Brown (1987), by permission

Figure 2.54). The individual internal processes in this particular volcano can be clearly differentiated by using the ratio of the gravity effects measured at the volcano flank and summit. However, not all sub-terrainian activity is associated with seismic signatures. Indeed,

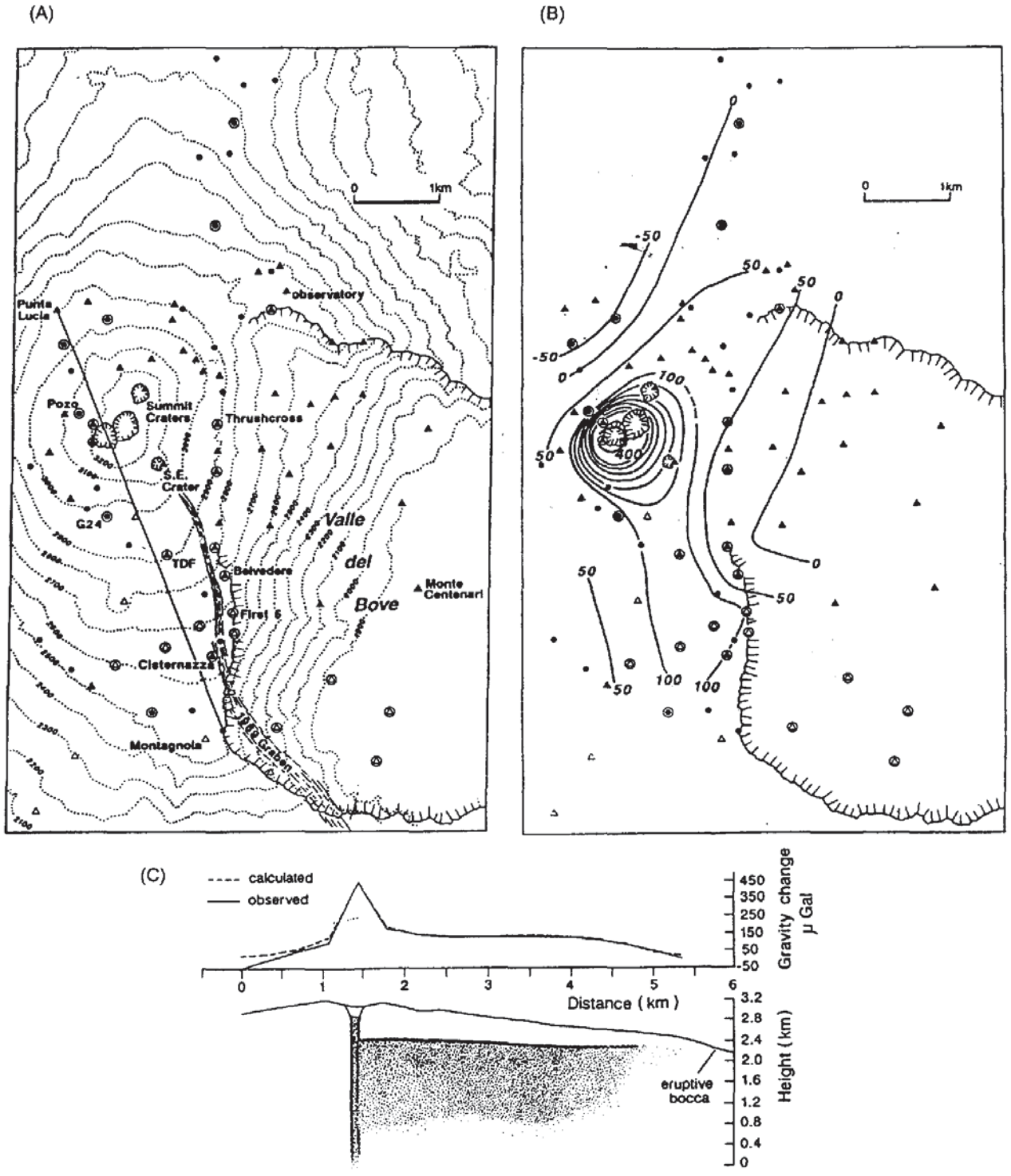

Figure 2.55 Maps showing (A) the locations of micro-gravity and ground deformation monitoring stations and (B) a contoured micro-gravity map of the summit area of Mt Etna, Sicily. The contour interval is 50 μGal. (C) Cross-section through the summit area of the Mt Etna along the profile indicated in (A). The best-fitting model for the observed gravity changes involved a dyke 4 m wide and a feeder pipe 50 m in diameter filling with magma at some time between the two sets of observations in June 1990 and June 1991. From Rymer (1993) and Rymer *et al.* (1993), by permission

Rymer (1993) reported on an increase in gravity at Mt Etna between June 1990 and June 1991 with no corresponding seismic activity. Large increases in gravity were observed around the summit craters and along an elongated zone following the line of a fracture formed during a previous eruption in 1989 (Figure 2.55). Surface elevation changes surveyed between 1990 and 1991 were only of the order of less than 3 cm. The gravity changes were an order of magnitude larger than would have been expected on the basis of elevation changes alone, which suggested that there must have been some sub-surface increase in mass. This was calculated to be of the order of 10^7 Mg and was caused by the intrusion of magma into fractures left by the 1989 eruption. The magma migrated passively into the pre-existing fractures so there was no corresponding seismic activity. Consequently, the micro-gravity measurements, in conjunction with elevations surveys, produced the only evidence of an impending eruption. The eruption of Mt Etna lasted for 16 months from 1991 to 1993, during which time lava poured out of the vent at a rate of $10\,m^3/s$, making this the largest eruption there for 300 years (Rymer 1993; Rymer *et al.* 1993).

Micro-gravity monitoring coupled with the distinctive patterns of the frequency of seismic activity (volcanic tremor spectra) are beginning to provide a very comprehensive model for volcanic eruptions, such as those at Mt Etna, and their associated processes. Many other volcanoes now have active monitoring programmes utilising gravity, seismic, and thermal investigations. Monitoring gas emissions is also proving to be a valuable additional indicator of impending volcanic activity (e.g. Pendick 1995, on the work of S. Williams). If these data can be obtained for individual volcanoes in conjunction with thermal radiation as measured by satellite, then the probability of identifying recognisable precursors to eruptions may be enhanced significantly, leading to a better prediction of volcanic activity and mitigation of potential hazards (Rymer and Brown 1986; Eggers 1987).